JMEPEG (2012) 21:1076–1084
DOI: 10.1007/s11665-011-9975-3

1059-9495/$19.00

Metallurgical Analysis of Ball Bearing Seized During Operation

Abhay K. Jha, M. Swathi Kiranmayee, P. Ramesh Narayanan, K. Sreekumar, and P.P. Sinha

(Submitted September 29, 2010; in revised form April 26, 2011)

440C stainless steel of martensitic grade is being extensively used for bearing application because of its high wear and corrosion resistance. This alloy steel with 1 wt.% C along with 17 wt.% Cr, 1 wt.% Mn and up to 0.75 wt.% Mo has a number of primary carbides, which provide high hardness and good wear resistance. Owing to its unique performance characteristic, this steel finds a number of applications in space program. One such application is bearing used in booster pump assembly of propulsion system. During one of the ground tests of propulsion system, booster pump bearing seized operation after performing its partial intended function. The bearing was removed from the assembly and cut open. The ball and outer caging were analyzed using metallographic techniques and compared with another bearing taken from the fresh stock. Study indicated that ball as well as outer caging experienced exposure to high temperature and resulted in phase transformation. This article highlights the details of investigations carried out.

Keywords aerospace, failure analysis, metallography

1. Introduction

High yield strength and good wear resistance of hypereutectic steels in hardened and tempered condition have made them attractive materials of choice to manufacture rotating parts of mechanical systems. Though impact toughness was poor, they were used as bearing material for a long period in the past.

However, improved toughness could be obtained in bearing made of 4620 steel by carburizing the case. Carburized case containing tempered martensite with small amount of retained austenite and a minor constituent of FCC alloy carbides have made these steels more attractive as bearing material. However, this had poor corrosion resistance and hence limited their use for critical applications. It is well known that corrosion resistance of steel can be increased by addition of minimum of 12% Cr. The need for a material with improved strength, wear resistance and corrosion resistance for bearing application resulted in the design of new steel having 17 wt.% Cr, up to 0.75 wt.% Mo and 1 wt.% C, which was christened as 440C.

440C has more primary carbides as compared to plain carbon steel or carburizable steel. These carbides large M_7C_3 (orthorhombic) and smaller $M_{23}C_6$ (FCC) are found in both annealed and quenched conditions. This alloy steel exhibited satisfactory results, especially at intermediate temperatures. However, due to high heat resistance, their use at high temperature is limited.

Abhay K. Jha, M. Swathi Kiranmayee, and **P. Ramesh Narayanan**, Material Characterisation Division, Vikram Sarabhai Space Center, Trivandrum 695 022, India; **K. Sreekumar**, Materials and Metallurgy Group, Vikram Sarabhai Space Center, Trivandrum 695 022, India; and **P.P. Sinha**, Materials and Mechanical Entity, Vikram Sarabhai Space Center, Trivandrum 695 022, India. Contact e-mails: ak_jha@vssc.gov.in and swathi_kiranmayee_manchili@vssc.gov.in.

440C stainless steel of martensitic grade is being used for almost all the bearing applications of Indian Space program. During one of the ground tests of a propulsion system, the booster pump bearing seized operation after completing the operation partially, because of interruption in fuel supply to the engine combustion chamber, and the test was aborted by itself. The bearing was found jammed during the post test inspection. The bearing was removed from the booster pump assembly and cut open. This bearing was subjected to Metallography analysis. Microstructural comparison was made with a new unused bearing. This article highlights the details of investigation carried out.

2. Material

The balls and bearing outer cage were fabricated out of 440C steel and were hardened and tempered to have hardness of 59 HRc.

3. Observations

The ball and outer caging of seized bearing henceforth will be referred as B_s and C_s, respectively, and the new unused fresh one as B_f.

3.1 Visual Inspection

The B_s had dull appearance, as compared with the appearance of B_f, which had bright appearance. The C_s had severe mechanical damaged region at location of ball-cage contact surface. Surface of the ball had a dent.

3.2 Scanning Electron Microscopy

Surface morphology of B_s, studied using Carl-Zeiss make EVO-50 scanning electron microscope (SEM), revealed that the

ball had undergone severe damage under mechanical loading and resulted in material spalling (Fig. 1). The outer caging also revealed similar surface rupture (Fig. 2). Dents created by the ball in contact with outer caging, under excessive mechanical loading ruptured the material adjacent to this (Fig. 2a). Isolated locations had features indicative of material exposed to very high temperature near or beyond its melting point (Fig. 2b, c). Multilayer delaminations, as shown in Fig. 2(d), indicated severe mechanical loading condition.

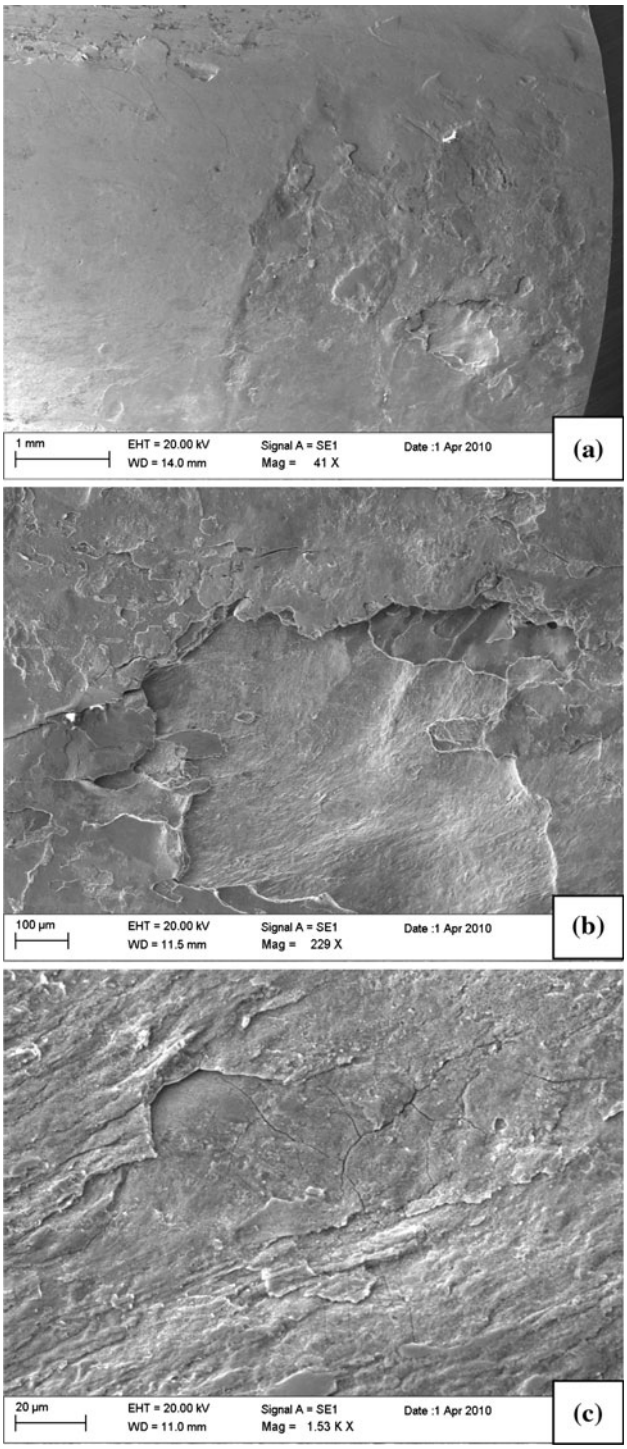

Fig. 1 Surface of ball seized during operation "B_s". (a) Severe damage under mechanical loading at different locations (b, c)

Figure 3 shows the cross section of the ball bearing. Cross section of C_s was sliced across the thickness and prepared for metallography. The prepared specimen indicated delaminated layer within 100-µm depth (Fig. 4) from the ball-outer cage contact point. Delaminated layer exhibited localized material deformation line within it (Fig. 4c, d).

3.3 Optical Microscopy

The balls B_s & B_f were cut into two halves and microstructure at the bi-sectional plane of each ball was studied. The microstructure was observed using an Olympus GX-71 inverted optical microscope. Microstructure consisted of fine-tempered secondary carbide particles in martensite (Ref 1). A narrow white band of 180-µm length was seen on peripheral region of B_s with an adjacent dark-etched region of 140-mm width (Fig. 5) with clear interface between the white narrow band at extreme periphery and dark-etched region. Dark-etched region had coarser white islands in the matrix of tempered martensite (Fig. 6). These white islands were thought to be coarser secondary carbides. Hetzner and Geertruyden (Ref 2) made similar observations and identified them to be M_7C_3 and $M_{23}C_6$ through X-ray diffraction. However, few isolated islands with morphological differences with that of secondary carbides were also seen, which were found to be reverted austenite. The B_f was devoid of these microstructural details (Fig. 7).

Cross section of C_s, duly polished and etched revealed similar features as seen on B_s. Dark-etched region was like necklace around the cavity of ball-cage contact region and had width of 600 µm at center and narrowing down at both the ends (Fig. 8).

Etching with Groesbeck's reagent gave better contrast to the microstructural details. The Fe_2MoC and M_6C were outlined and colored blue and brown, respectively (Ref 2) as seen in dark field optical images. These carbides were coarser and non-uniformly distributed within the dark-etched region (Fig. 9), while they were fine and more uniformly distributed within the remaining material of the ball (Fig. 10).

3.4 Microhardness

Microhardness measurements were carried out using CLEMEX make CMT microhardness tester with 500 g load on bi-sectional plane of both the balls i.e., ball B_s and B_f. The measurements were carried out on ball (B_s) from outer periphery through dark-etched region to the core of the ball material. Hardness values were measured at various locations and plotted. *X*-axis represented distance in mm with zero point as outer edge. There was a distinct drop in hardness within the dark-etched region (Fig. 11), in comparison with minimum acceptable hardness value of 700 VHN at 500 g load which is equivalent to 59 HRc, while it was more or less uniform for B_s. Similar drop in hardness within dark-etched region was noticed in C_s (Fig. 12).

3.5 Energy Dispersive Spectrum (EDS)

Microstructure in the core region of B_s revealed unresolved martensite (Fig. 13a) in general with fine carbide particles. Within the dark-etched band, Over tempered martensite matrix (Fig. 13b) was seen with coarse carbide particles. EDS of carbide and matrix is shown in Fig. 14. Similar observations were made on C_s.

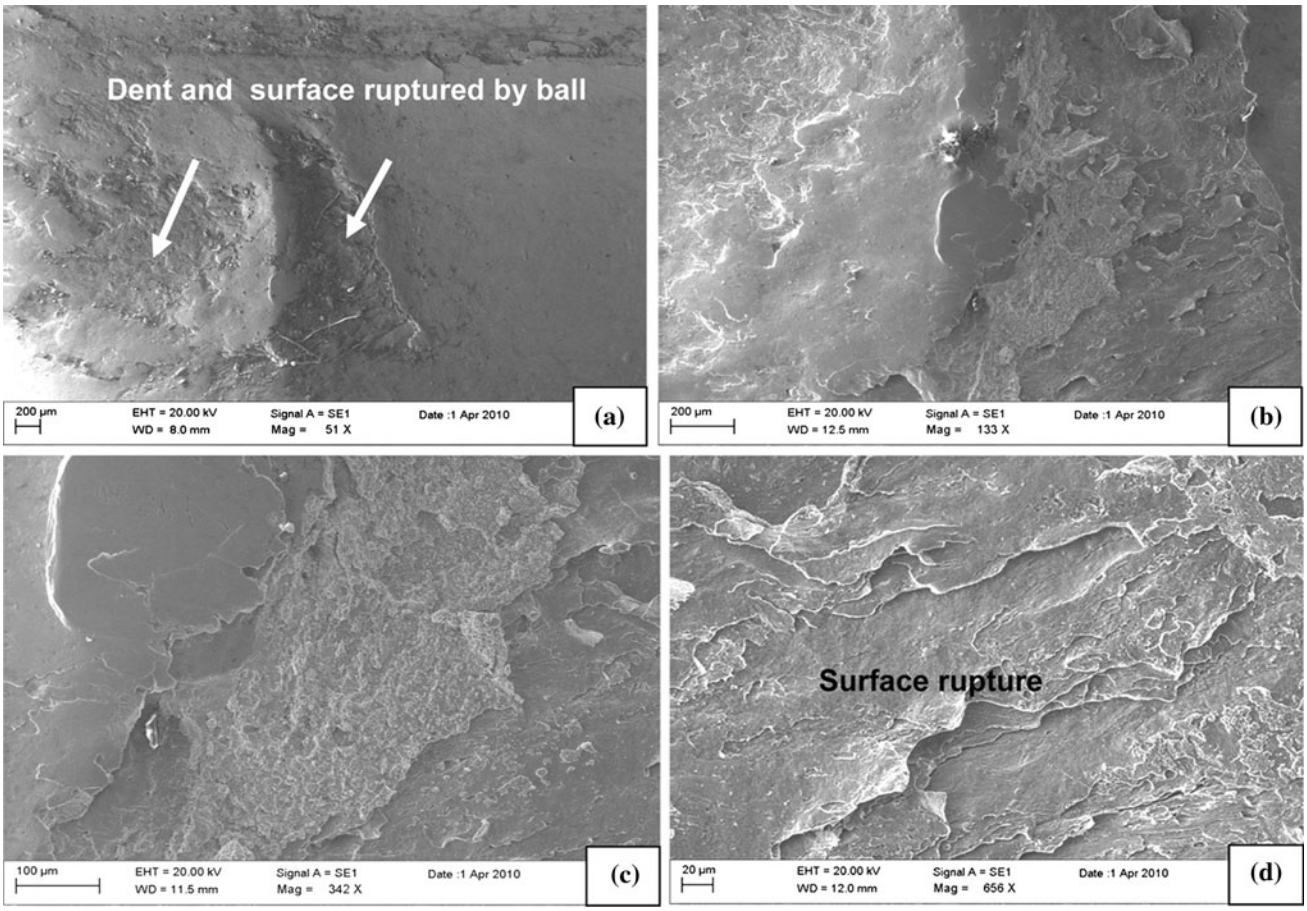

Fig. 2 Features of slotted region of case "C_s", which was in contact with ball motion (lateral surface). (a) Dent at ball contact point; (b, c) smooth surface feature; (d) surface rupture point

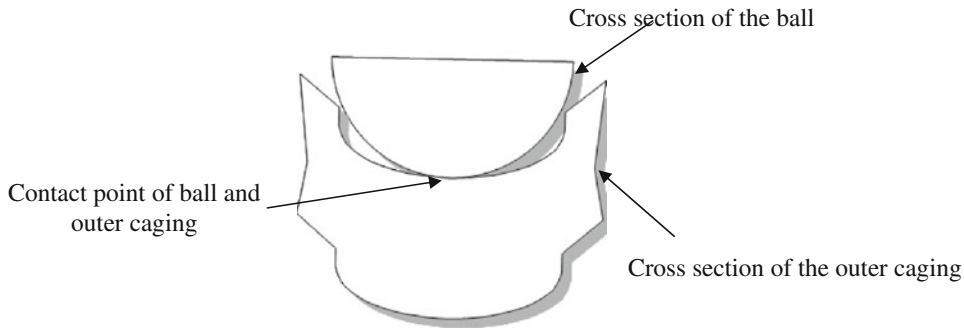

Fig. 3 Cross-section of the ball the bearing showing ball and the outer caging

3.6 Differential Scanning Calorimetry (DSC)

Sample of 3-mm diameter and 0.5-mm thick disc made out of C_s was subjected to DSC from RT to 800 °C with heating rate of 10 °C per min and 800-950 °C, with heating rate of 5 °C/min. Slower heating rate at elevated temperature was chosen taking into consideration 17 wt.% Cr Isopleth, Fe-Cr-C phase diagram (Fig. 15). Heating rate was kept as low as 5 °C per min during temperature range of 800-950 °C. DSC curve (Fig. 16) confirmed endothermic phase transformation (Ferrite → Austenite) at the temperature of 840 °C, which was in good agreement with Fe-Cr-C phase diagram.

4. Discussion

The bearing seized during its use and after performing operation for a reasonable time. Observations revealed severe mechanical deformation on either B_s or C_s. The delaminated layers had indication of severe localized mechanical deformation of the material. The dark-etched region B_s was attributed to its exposure to high temperature during operation or rather hindered operation. There may be many reasons for the loss of the rotational attitude, which represents the major functional requirement of bearing component. Mapelli and Barella (Ref 3)

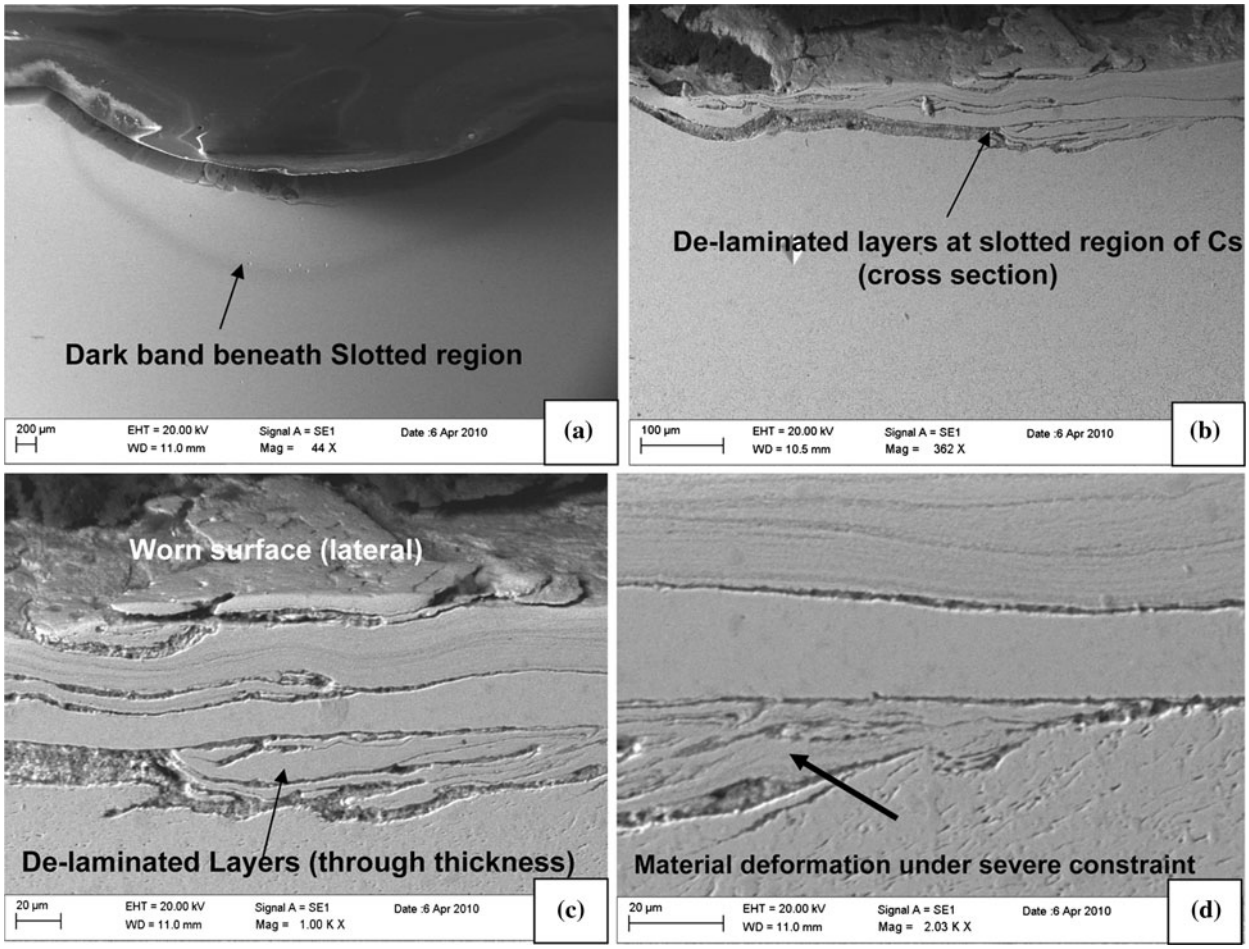

Fig. 4 Features at slotted region of C_s, which was in contact with ball motion (cross section, i.e., through thickness). (a) Dark band; (b-d) delaminated layers

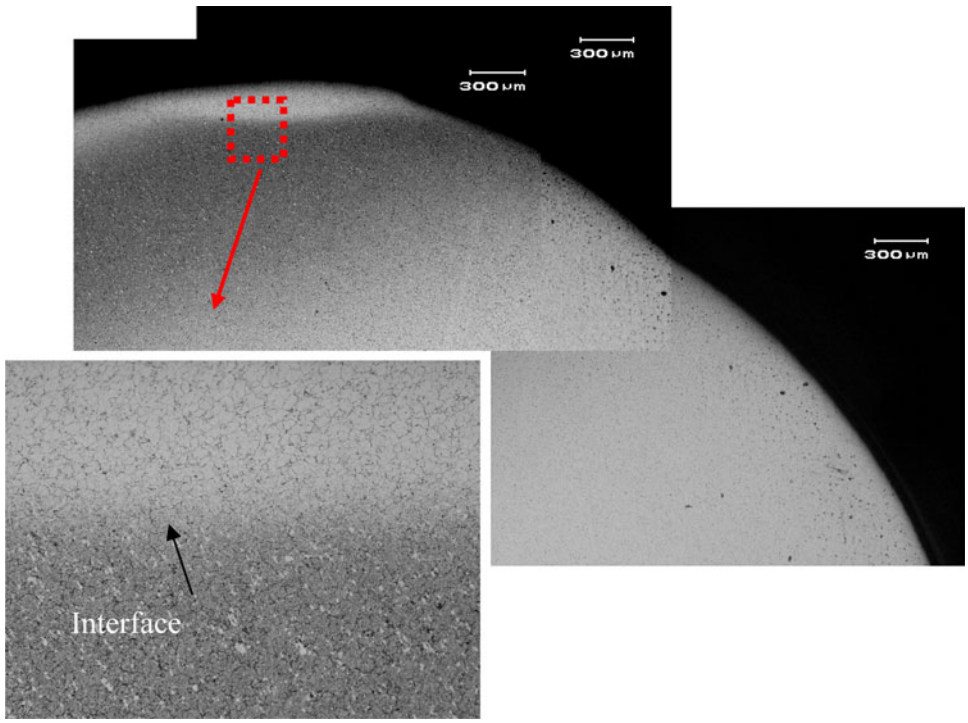

Fig. 5 Interface between the dark band and light region [*etchant*: Villela's reagent (5 mL HCl, 1 g picric acid, and 100 mL methanol)]

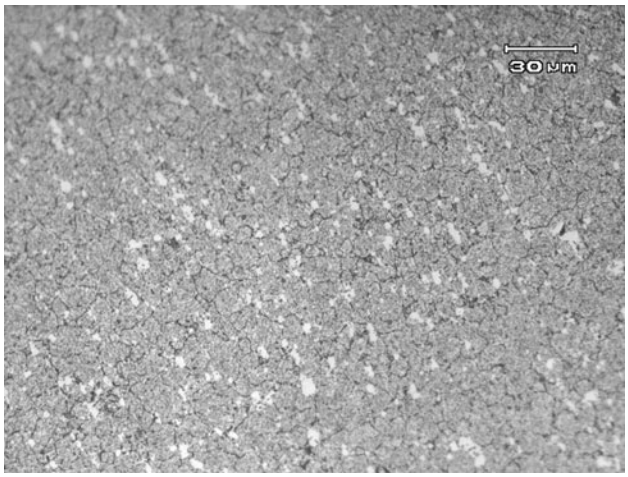

Fig. 6 Structure in the dark band region [*etchant*: Villela's reagent (5 mL HCl, 1 g picric acid, and 100 mL methanol)]

identified abrasive body debris of exogenous origin as major cause for loss of rotational attitude of bearing component. However, to identify the cause of bearing seizure is beyond the scope of this study. The characteristics of both the B_s and C_s revealed drop in hardness within a narrow dark band near contact point, while it was uniform for B_f.

Temperature rise in ball material due to friction loss is very common, and the amount of thermal energy generation caused by friction moment can be calculated using formula:

$$Q = 0.105 \times 10^{-6} MN$$

where Q is the thermal value (kW), M the friction moment (N mm), and N is the rotational speed (rpm),

The operating temperature of a bearing is determined by the equilibrium or balance between the heat generated and that conducted away from it. In most cases, the temperature rises sharply during initial operation, then increases slowly until it reaches a stable condition and then after remains constant. This is ideal operating condition of a bearing. However, if it

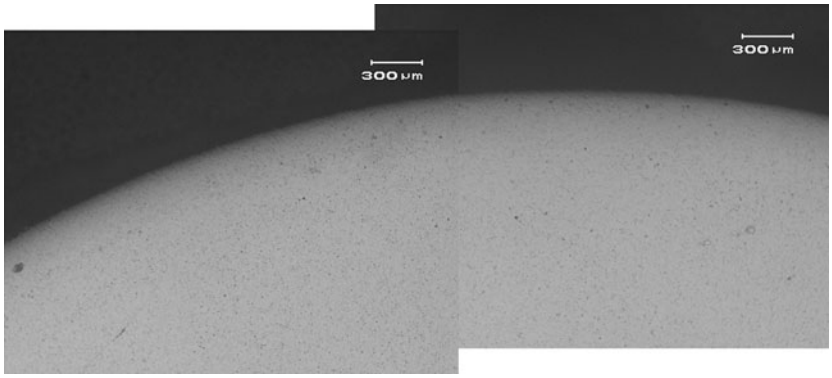

Fig. 7 Optical photomicrograph showing the absence of dark band in ball (B_f)

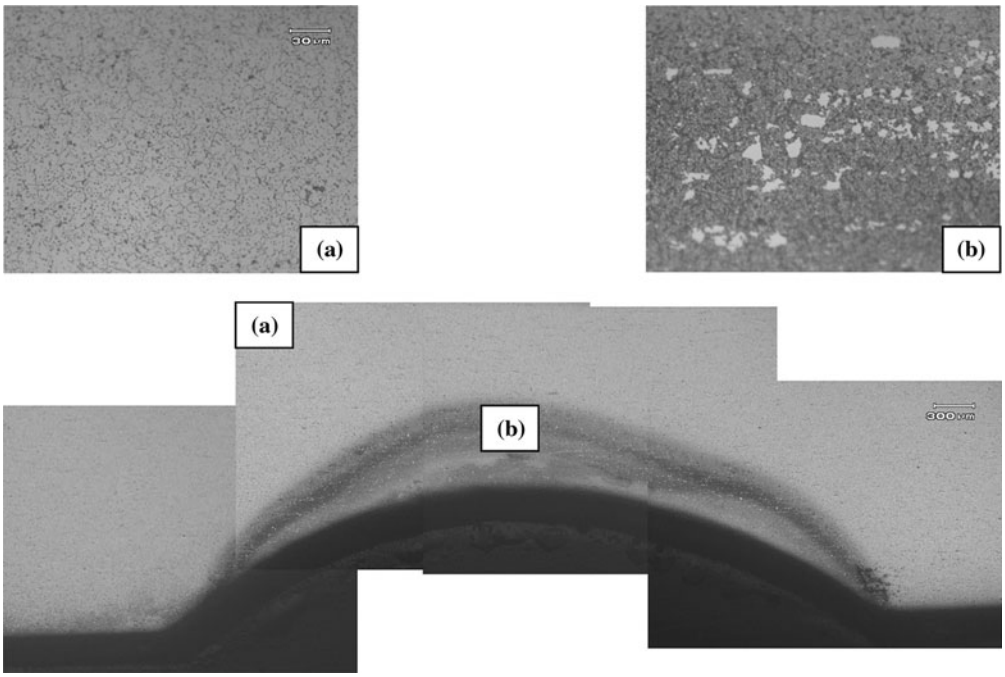

Fig. 8 Optical photomicrographs of outer caging (C_s) showing dark band as necklace. (a) Core region; (b) dark-etched band region [*etchant*: Villela's reagent (5 mL HCl, 1 g picric acid, and 100 mL methanol)]

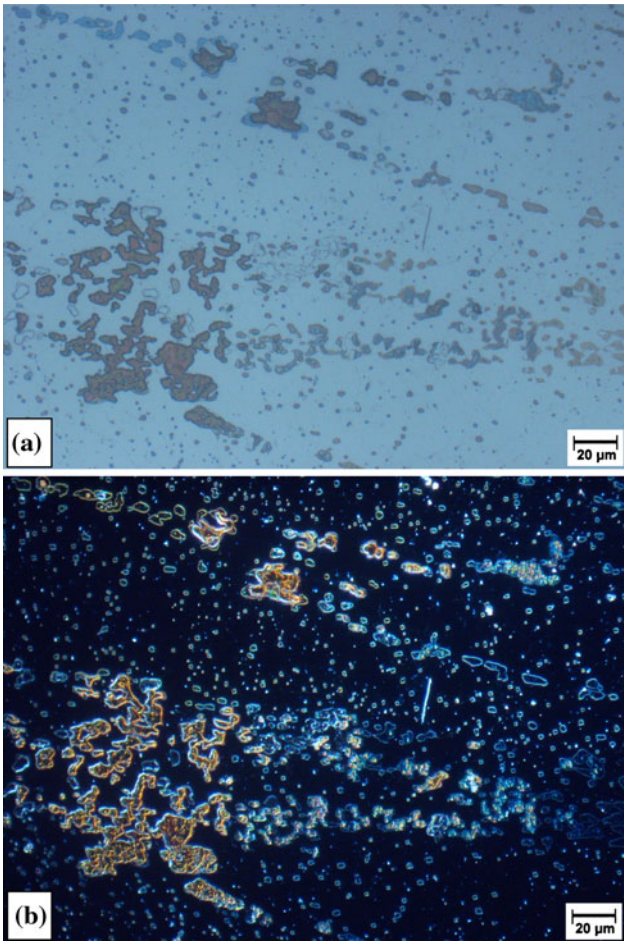

Fig. 9 Optical photomicrographs of dark etched region near outer periphery of ball 'B_f' showing carbides duly color etched: (a) bright field; (b) dark field [*etchant*: Groesbeck's reagent: 4 g $KMnO_4$ + 4 g NaOH + 100 mL H_2O at 20 °C]

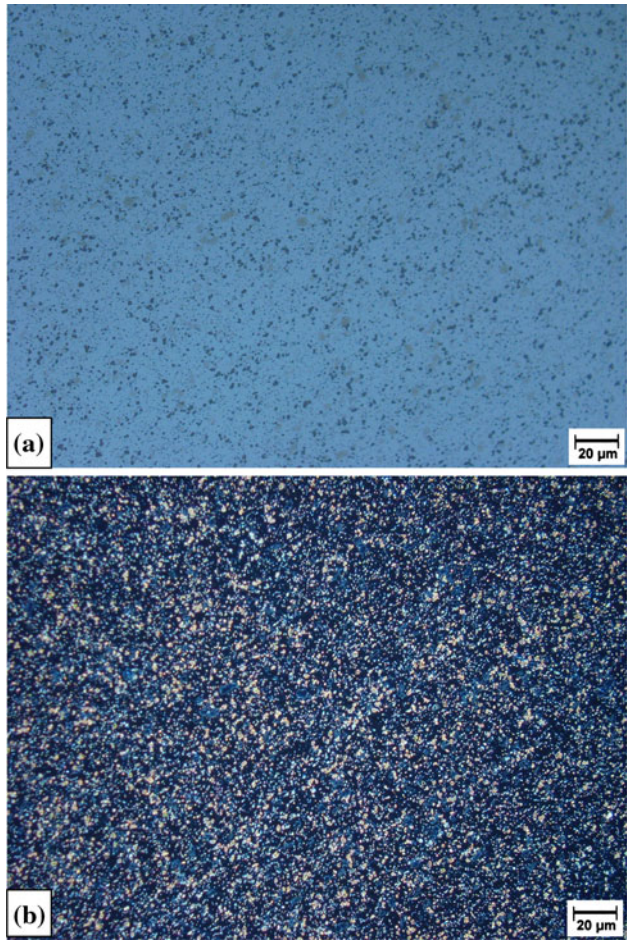

Fig. 10 Optical photomicrographs at core of ball 'B_f' showing carbides duly color etched: (a) bright field; (b) dark field [*etchant*: Groesbeck's reagent: 4 g $KMnO_4$ + 4 g NaOH + 100 mL H_2O at 20 °C]

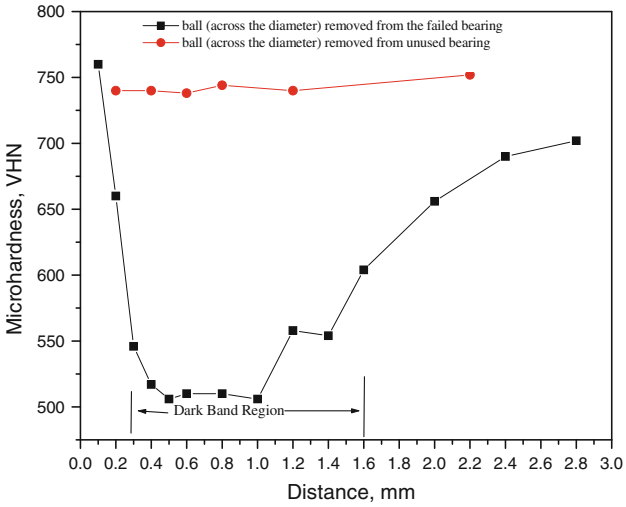

Fig. 11 Microhardness profile of B_s and B_f

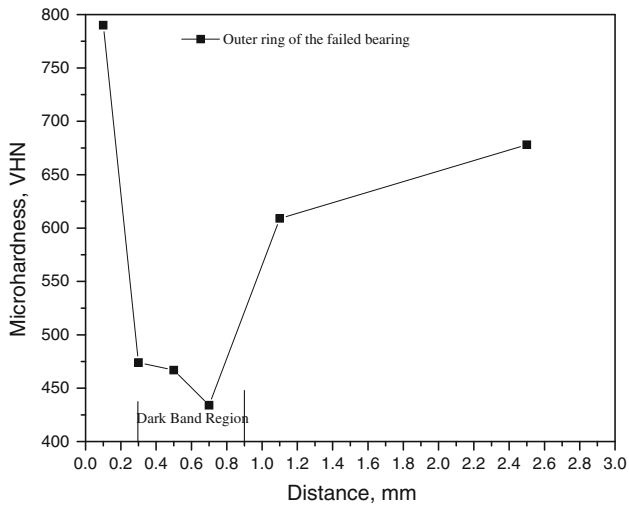

Fig. 12 Microhardness profile of C_s (cross section)

malfunctions, temperature continues to rise without reaching a stable state. The reasons for such improper function may be moment load, insufficient internal clearance, excessive preload, too little or too much lubricant, foreign matter in the bearing, or heat generated at the sealing device. Any one or more of the above is sufficient to generate excessive high temperature to the ball and even the outer ring.

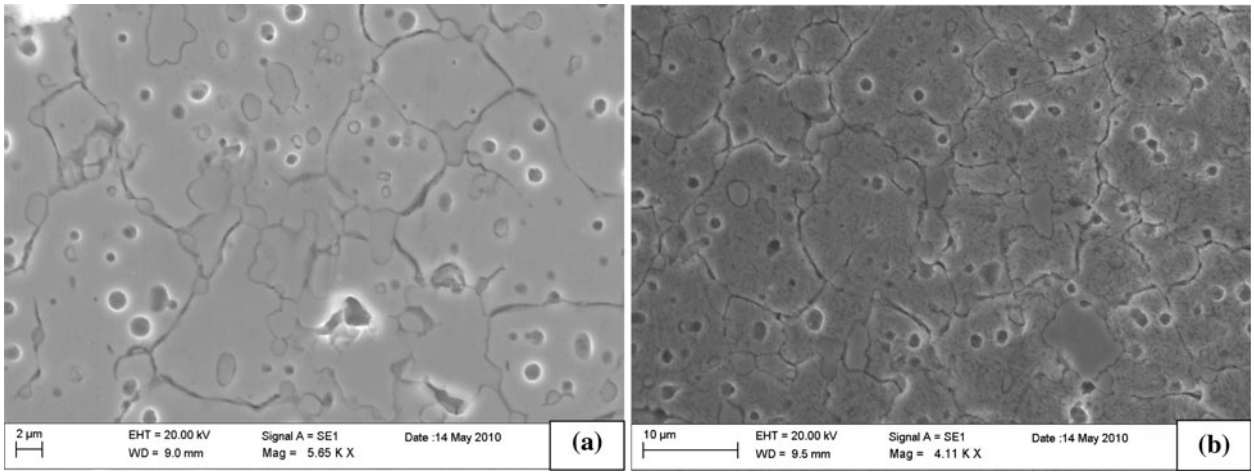

Fig. 13 SEM photomicrographs revealing the microstructure in etched condition. (a) In the core of the ball; (b) in the dark-etched band region

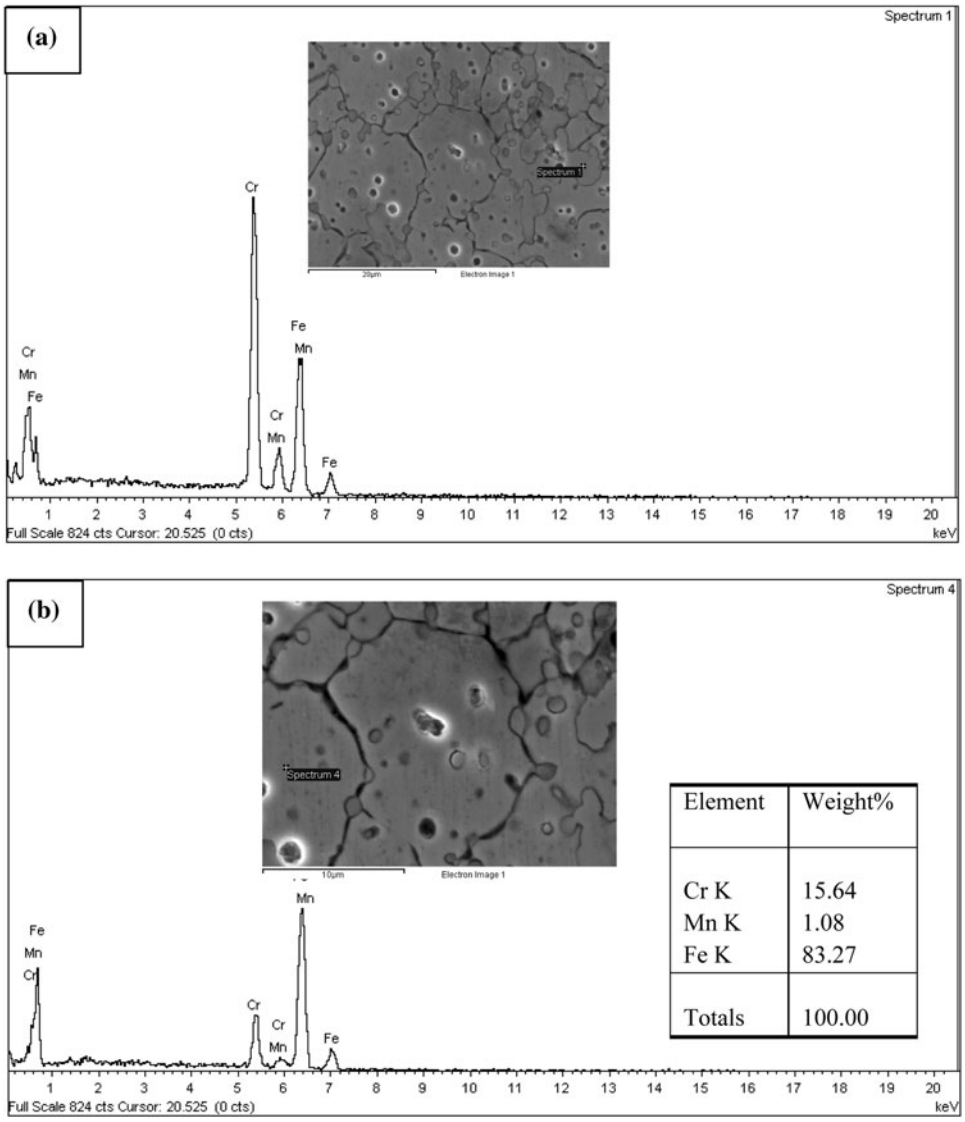

Fig. 14 EDS spectrum (a) on the chromium carbide particle; (b) on the matrix

Many researchers (Ref 4, 5) have observed high contact temperature during malfunctioning of the bearing. Further Carpenter et al. (Ref 6) have reported excessive temperature rise during seizure of a freight car bearing. While in some of the cases (Ref 7), the thermal flux generated was enough to melt the material.

Based on 17% Cr Isopleth, Fe-Cr-C phase diagram (Fig. 14), 440C appears to be relatively less complicated. On heating to 1050 °C, primary constituents are austenite, M_7C_3 and $M_{23}C_6$. Quenching to room temperature, followed by tempering results in tempered martensite, consisting of these carbides and less amount of retained austenite.

In the present case study, we could not get clear evidence of melting. However, based on evidences, reaching very high temperature near melting points could not be ruled out. The narrow white band at a localized peripheral region of ball taken out from seized bearing component was indicative of attaining temperature above austenization temperature which got cooled/quenched rapidly as the remaining material behaved as heat sink. Such condition developed untempered martensite phase (Ref 8). The marginal higher hardness of this layer (740 VHN on 500 g load) than the core of B_s (700 VPN on 500 g load) with tempered martensite was due to this thin layer of untempered martensite. This layer is brittle and gets fragmented easily. The fine cracks at outer peripheral layer of B_s were the result of such brittle untempered martensite. Adjacent to this narrow white band of untempered martensite, there exists dark-etched region consisting of a number of coarse white islands in martensitic matrix. This was the region, which experienced temperature rise above 850 °C (Fig. 14) and there was every possibility of austenite reversion to take place. This can be explained as per 17% Cr Isopleth, Fe-Cr-C phase diagram (Fig. 14) and confirmed with DSC. However, possibility of existing carbides to grow (Ref 9) and coarsen could not be ruled out. In the present case study, coarsening of existing carbides within this dark-etched region was confirmative indication of the fact that material within this region experienced temperature above 850 °C. The B_s had microstructure unaffected, as temperature experienced was less than 800 °C and so. Similar was the observations on C_s also.

It could be concluded from the above observations that after performing a part of intended operation, balls lost their rotational attitude due to loss of clearance, caused excessive heat generation and resulted in seizure of its operation. Most probable cause for clearance loss was due to contaminant particles introduced in to the bearing gap. Bearing seizure of similar nature was reported by Frankline et al. (Ref 10).

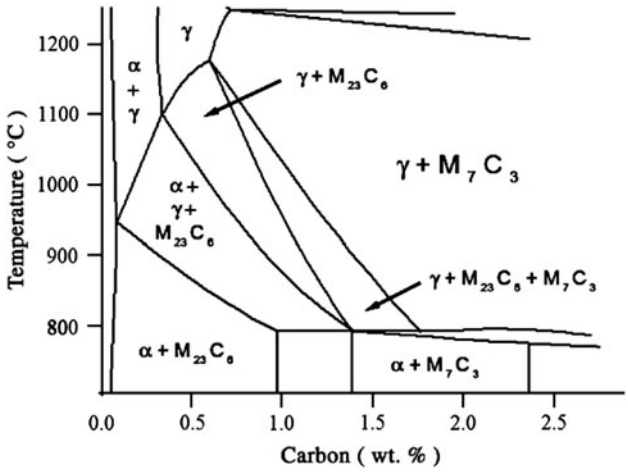

Fig. 15 17% Cr Isopleth, Fe-Cr-C phase diagram

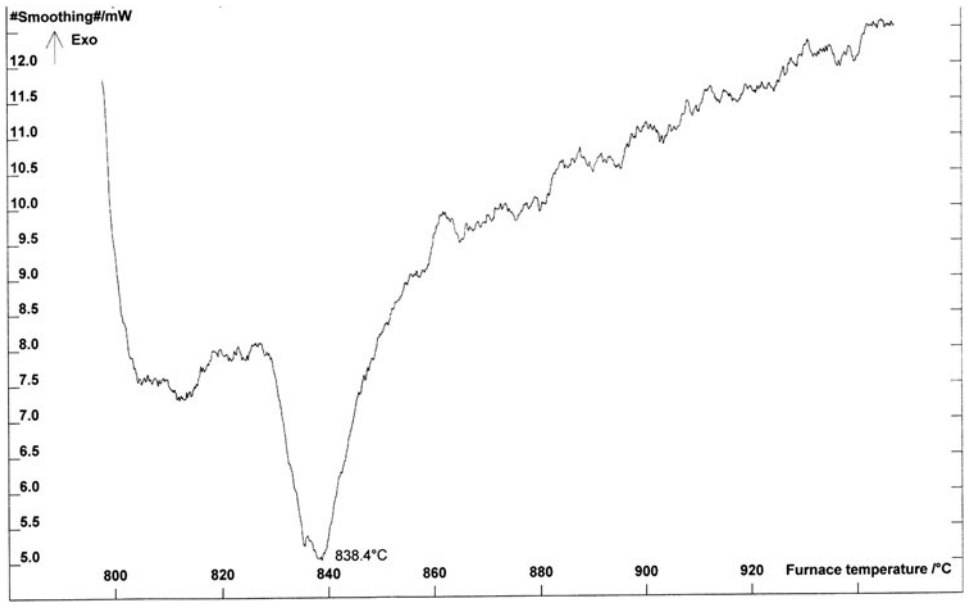

Fig. 16 DSC curve showing endothermic phase transformation

Acknowledgment

The authors are indebted to Shri P.S. Veeraraghavan, Director, VSSC for permission to publish this study.

References

1. T. Lyman, Ed., *Metals Hand Book*, Vol 7, 8th ed., ASM, Metals Park, OH, 1972, p 145
2. D.W. Hetzner and W. Van Geertruyden, Crystallography and Metallography of Carbides in High Alloy Steel, *Mater. Charact.*, 2008, **59**, p 825–841
3. C. Mapelli and S. Barella, Failure Analysis of a Ball Transfer Unit, *Eng. Fail. Anal.*, 2007, **14**, p 579–587
4. D.K. Chaudhuri, A.J. Slifka, and J.D. Siegwarth, Friction and Oxidation Wear of 440C Ball Beraing Steels Under High Load and Extreme Bulk Temperature, *Wear*, 1993, **160**(1), p 37–50
5. B. Vick, M.J. Furey, and K. Iskandar, Surface Temperature Generated by Friction with Ceramic Materials, *Tribol. Trans.*, 1999, **42**(4), p 888–894
6. G.F. Carpenter, M.W. Joerms, W.H. Sheed, K.L. Hawthorne, and D.H. Stone, Theoretical and Experimental Determination of Heat Flow into a Wheel Due to Bearing Overheating, *IEEE/ASME Joint Railroad Conference*, 25th April 1989 (Philadelphia, PA, USA), 1989
7. M. Ristivojevic, R. Mitrovic, and T. Lazovic, Investigation of Causes of Fan Shaft Failure, *Eng. Fail. Anal.*, 2010, doi:10.1016/j.engfailanal2010.02.004
8. H.E. Boyer, Ed., *Metals Hand Book*, Vol 10, 8th ed., ASM, Metals Parks, OH, 1975, p 461
9. A.K. Jha, K. Sree Kumar, T. Thomas, and P.P. Sinha, Process Optimization for High Fracture Toughness of Maraging Steel Rings Formed by Mandrel Forging, *J. Manuf. Process*, 2010, **12**, p 38–44
10. S.M. Franklin, R.W.M. Severt, and J.B. Post, Improvement of the Seizure Resistance of Orifice-type Aerostatic Bearings (Case Study), *Wear*, 2006, **261**, p 41–45